Full Research Program

Plasmonic Metasurfaces with broken space-inversion symmetry: From geometric Berry phase to topological plasmonics

Gorodetski Yuri

1 Scientific background

Two-dimensional (2D) materials have been of great interest since the discovery of graphene. In recent years, the field has developed rapidly with the discovery of many types of 2D materials such as transition metal dichalcogenide (TMD) monolayers.[1–5] Due to their unique physical properties and a broad potential applications, research has focused on the fabrication and underlying physics of TMDs. TMDs are semiconductors of the form MX_2 where M is a transition metal atom such as Mo or W and X is a chalcogen atom such as S, Se, or Te. When cleaved to a monolayer, these materials exhibit a direct band-gap, strong spin-orbit coupling, and favorable electrical and mechanical properties. Thus, TMDs such as $M0S_2$ have a valley degree of freedom, enabling the development of valleytronic devices.[6] TMDs also possess topological phases due to their symmetry, giving rise to a non-trivial Berry phase. Many TMDs behave as topological insulators (TIs) hosting topologically protected conducting-edge states.[7,8] These and other unique features of the 2D materials have found a vast variety of applications in nanoelectronic and electrooptics which reinforces the importance of deeper study of the related fundamental physical processes.

The Berry phase[9] is a phase added to an eigenstate after completing a closed loop in the parametric space in which it is defined.[10] It is caused by non-trivial topology of the state-space and often called a “geometric phase”.[11,12] In crystals of broken time-reversal or space- inversion symmetry, the level degeneracy of chiral eigenstates (quasi-spins) is lifted. This lift gives rise to the so-called Berry curvature which is comparable to the appearance of magnetic monopoles.[13] In symmetric structures such as graphene, time-reversal symmetry can be broken using a strong magnetic field. TMDs such as MoS_2 and WSe_2 have a hexagonal lattice structure similar to that of graphene; however, the different atoms within the honeycomb unit cell break inversion symmetry. Therefore, the Berry phase accumulated by Bloch electrons at their Dirac points, which are degenerate in graphene, are of opposite sign making the K and K' valleys distinguishable.

It has been shown repeatedly that light modes propagating in a periodically modulated space can exhibit behavior analogous to electronic wave-function in a crystal.[14,15] The parameter space

that defines the state of polarized light is the Poincaré sphere, where the north and south poles correspond to right- (RCP) and left-hand circular polarization (LCP), respectively. A cyclic change of the polarization state induces a measurable and helicity-dependent Pancharatnam-Berry (PB) phase.[16,17] This phase is equal to half of the solid angle enclosed by the loop. The PB phase is responsible for the spin-Hall effect of light[12,18] and has played an important role in numerous applications in optics[19,20] and plasmonics.[21–23]

Here we consider plasmonic PB phase metasurfaces with graphene-like structures but with broken inversion symmetry. Plasmonic metasurfaces with subwavelength space-variant anisotropic scatterers have been shown to produce the PB phase.[22,24] Such structures have been used for spin-dependant directional excitation of surface plasmon (SP) waves and have been the subject of much research[25–27] due to their potential in development of nano-photonic devices. By measuring the plasmonic response upon illumination with different spin states in momentum space, we show that the excited plasmonic modes strongly depend on the helicity of the incident light. Explicitly, we observe a spin-degeneracy lifting analogous to the behavior of TMDs at their K and K' valleys. In our case, inversion symmetry is broken by angular difference between adjacent apertures in the metasurface. This angle leads to opposite PB phases in the K and K' points in momentum space, resulting in a contrast between the two circular polarizations in both the near and far field. This contrast is then varied by controlling the aperture angle. These results are consistent with numerical calculations that we performed.

Interestingly, it seems that an analogy can be drawn between our structures and 2D materials such as TMDs. Both have a graphene-like structure but with inversion symmetry broken. As mentioned above, this broken symmetry causes a strong spin-orbit interaction and the occurrence of a Berry phase. The plane separation between the constituent atoms in the unit cell can be associated with the rotation of the apertures in our metasurface. The pseudospin accounting for the rotational motion of electrons within the honeycomb unit cell is just like the SP waves circulating in the unit cell of our structure, following the path of constructive phase building. It has been shown that optical topological phases can model complex quantum systems.[28] Much theoretical insight can be gained from such analogies. Although the fabrication of 2D materials is improving rapidly, it currently remains a complicated procedure. Our structures, by contrast, are easy and cheap to prepare, as well as being very flexible having many parameters to play with. Measuring and analyzing our system is also very straightforward with many degrees of freedom. We thus propose a simple way to analyze optical properties of TMDs and possibly make predictions of yet unknown features.

If this connection could be shown theoretically, this could open many doors to further deepening of our understandings of TMDs.

2 Research objectives and expected significance

Numerous analogies have been recently demonstrated between the behavior of electrons and photons in periodic media. Electronic band structure, that mainly determines the electromagnetic properties of the material can be compared to the photonic band structure in so called “photonic crystals” which imposes most of the optical properties of the medium. For instance, materials with well-pronounced electronic band-gap appear as electrical insulators, while opening a photonic band-gap leads to the full reflection of the photons withing the gap frequency range. The significance of this research is to establish a theoretical connection between the spin-dependent electronic effects in TMDs and plasmonic effects in metasurfaces with broken inversion symmetry. The specific research objectives leading to this goal are listed below.

Objective 1. Investigation of the spin-dependent plasmonic effects in the vicinity of the K, K’ points.

We propose investigating the effect of inversion symmetry breaking in periodic and quazi-periodic plasmonic metasurfaces in terms of spin-dependent energy distribution and flow, especially in the regions of k-space near the K, and K' points of the Brillouin zone. It has been already shown (see the Preliminary results section), that spatially rotated apertures arranged in a honeycomb lattice induce spin-dependent unidirectional excitation of SPs due to the Berry phase. A graphene-like structure, defined as a composition of two honeycomb sub-lattices exhibits much richer physics resulting in a polarization dependent photonic band-gap. The dependence of this band-gap on structure geometry, its properties and effects on other photonic phenomena will be studied in detail in plasmonic structures. The metasurfaces will be first analyzed numerically by a commercial software as well as by using a specifically built semi-analytical model. Next, we plan to design and nanofabricate the structures using existing facilities (described in Current Research Facilities section) and experimentally study the plasmonic behavior in the real and the k-spaces.

Objective 2. Plasmonic edge states.

In analogy with TMDs and other semiconductors exhibiting topological effects we propose to investigate the prerequisites for the excitation of the plasmonic edge modes along the boundaries

of metasurface. As we show here in the Preliminary results section, we have observed plasmonic mode localization about the edges of some specific graphene-like structures, which, we believe, have topological origin. Nevertheless, more study is needed to characterize these phenomena it terms of the dispersion relation, topological protection, robustness to scatterings etc. We plan to develop analytical models predicting plasmonic edge states and to experimentally investigate these modes. With better understanding of the underlying physical mechanism we expect to further investigate complex structures comprised of domains with different topological properties and their capability to localize and guide SPs.

Objective 3. Investigation of plasmonic heterostructures with TMDs.

We propose to incorporate the basic models and the obtained experimental results to study the effects in complex systems comprising of a TMD layer stacked on top of the plasmonic metasurface. The interaction of the SP waves with the excitons in the TMD layer in different coupling regimes will be investigated. Recently, we have already shown that such interaction may lead to intriguing spin-based effects in the nanoscale. Here we suggest place different types of TMD on our graphene-like structures and experimentally study the plasmonic or excitonic modes excited in the device. We believe that topological plasmonic metasurfaces may reveal additional spin-selectivity and enhancement providing a novel degree of freedom in nanophotonics and electronics.

2.1 Working Hypothesis

We hypothesize that a plasmonic metasurface can demonstrate topological effects analogical to some 2D materials when the following conditions are fulfilled.

1 The space-inversion symmetry of the structure is broken. We believe that this induces spin-orbit coupling leading to unidirectional plasmonic modes localized about K and K’ points in the k-space.

2 The lattice is in the form of graphene structure and can be represented as a summation of two honeycomb sub-lattices. This reduces the mobility of the plasmons hoping between the apertures which results in a photonic bandgap.

Apparently, when these two conditions meet, the unit cell becomes genuinely chiral which is the main cause of the spin-dependent effects. Subsequently, the periodicity together with the relative aperture orientation angle may now be used to manipulate the topological order of the structure.

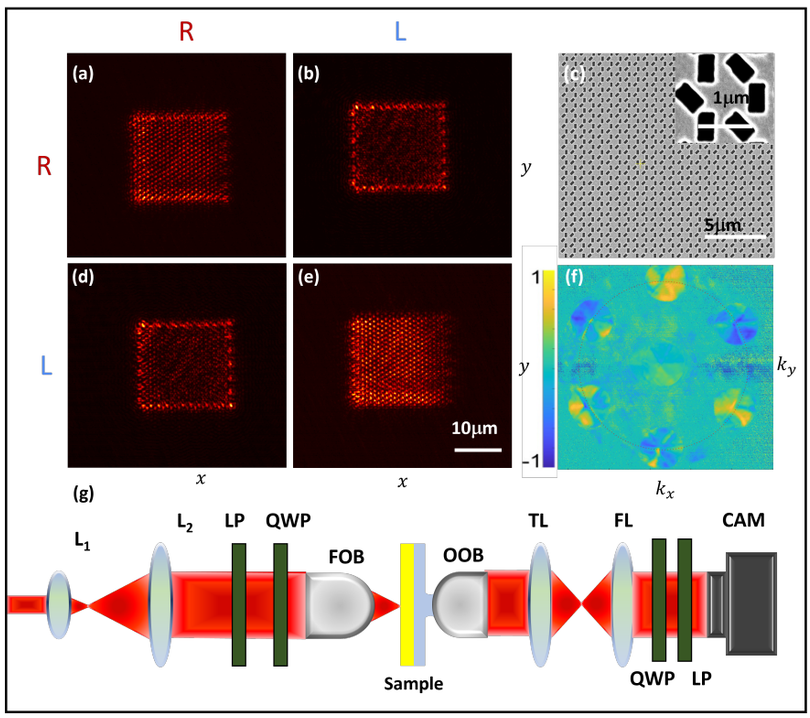

Figure 1: (a),(b),(d) and (e) Plasmonic spin-dependant edge-state at the boundary of a graphene-like metasurface when the output polarization differs from the input (input polarization arranged in rows and output in columns). (c) A SEM image of the metasurface with a close up of the unit cell in the inset. (f) Spatial CD map (in k-space) of the structure. The primary plasmonic resonance circle is marked by the dotted red line. (g) Schematic illustration of the optical setup consisting of lenses (L_1, L_2), a linear polarizer (LP),quater wave plate (QWP), focusing objective (FOB), oil-immersion objective (OOB), tube lens (TL), Fourier lens (FL) and a camera (CAM).

By testing these hypotheses, we will be able address the role of the inversion symmetry breaking in TMD structures as well as design and investigate analogical plasmonic metasurfaces.

3 Proposed research and preliminary results

Our metasurface is an array of rectangular apertures in a 100 nm thick gold film, arranged in a honeycomb lattice. The lattice constant is $a = 3\lambda_{sp}/4$, where λ_{sp} is the wavelength of the SP excited at the gold-air interface and is given by $\lambda_{sp} = \frac{2\pi c}{\omega}\sqrt{\frac{1+\epsilon_{Au}}{\epsilon_{Au}}}$, while $\epsilon_{Au}(\omega)$ is the dielectric function of gold at frequency ω. We rotated each of two neighboring apertures to an angle of $\theta = \pi/4$ between them. We used a laser diode at $\lambda_0 = 2\pi c/\omega = 780$ nm and, therefore, in our case, $a = 574$ nm. A scanning electron microscope (SEM) image of our sample is presented in Fig. 1c. The apertures were milled by using a focused ion beam (FIB) into the gold film evaporated on a glass substrate by sputtering. The laser beam was expanded then focused by a microscope objective ($NA = 0.25$) onto the sample at the air-gold interface. The back of the glass substrate was brought into contact with an oil-immersion objective ($NA = 1.3$) that collected plasmonic leakage radiation.[29] A tube lens then formed an image on the camera, with an additional (Fourier) lens using a flipped mount to image the k-space, as needed. The polarization state of the incident light

was controlled by a polarizer and a waveplate. The setup is illustrated schematically in Fig. 1g. The measurements were performed in real and reciprocal (k-space) spaces. In Figs. 1(a, b, d, and e), the real space distributions for the incident RCP and LCP light are shown as measured through a circular analyzer. We found that in the cases of crossed polarization (Figs. 1(b and d)), there was a strong localization of light along the circumference of the metasurface, whereas the outside and inside of the structure remained dark. When the output polarization was the same as the input (Figs. 1(a and e)), there was no special behavior and the light appeared to be transmitted by the structure. We further measured the response of the structure for both spin states (without polarization filtering at the output) in the k-space and calculated the circular dichroism (CD) of the structure, defined as

$$\Delta = \frac{\sqrt{I_R} - \sqrt{I_L}}{\sqrt{I_R} + \sqrt{I_L}} \tag{1}$$

where $I_{R,L}$ is the measured intensity for RCP and LCP illumination, respectively (Fig. 1f. K-space measurements are discussed later in greater detail. We note that the diffraction orders have a strong polarization dependence, whereas the central (zero) order near null CD. Specifically, we observe three predominantly LCP polarized orders; the other three are RCP. This spin-dependent k-space disctribution resembles excitonic directional propagation in TMDs. To understand the meaning of our measurements, we refer to the structure discussed in Ref. [27] (see the inset in Fig. 2). We consider a hexagonal lattice of rectangular apertures rotating along its primary directions. The rotation rates are defined by constants $N = 3$ and $M = -3$ (here N and M are the number of the grating periods needed to complete a rotation of n radians). The relative angle between the neighboring apertures is $\pi/3$ and the lattice constant is $a = 2\lambda_{sp}/3$. As discussed in detail in ref. [27], with these parameters, only three unidirectional plasmonic beams are excited for each circular polarization state. This strong polarization selectivity is achieved by the rotation-induced Coriolis term added to the momentum-matching condition, which leads to the PB phase.

Explicitly, a structure defined by the direct lattice primitive vectors $\mathbf{a} = a\hat{\mathbf{a}}$ and $\mathbf{b} = b\hat{\mathbf{b}}$ produces a diffraction pattern according to its reciprocal primitive vectors $\mathbf{a}^* = 2\pi\frac{\mathbf{b}\times\hat{\mathbf{z}}}{\mathbf{a}\cdot(\mathbf{b}\times\hat{\mathbf{z}})}$ and $\mathbf{a}^* = 2\pi\frac{\mathbf{a}\times\hat{\mathbf{z}}}{\mathbf{a}\cdot(\mathbf{b}\times\hat{\mathbf{z}})}$. However, the space-variant aperture rotation $\theta(x, y)$ (with respect to the y axis) leads to an additional term in the total grating momentum of $-\sigma\mathbf{k}_\Omega$. We define the Coriolis term $\mathbf{k}_\Omega = 2\Omega$, where $\Omega = \Omega_{\mathbf{a}}\hat{\mathbf{a}}^* + \Omega_{\mathbf{b}}\hat{\mathbf{b}}^*$ is the aperture rotation rate vector, $\Omega_{\mathbf{a}} = \nabla_{\mathbf{a}}\theta(x, y) = \frac{\pi}{Na}$ and $\Omega_{\mathbf{b}} = \nabla_{\mathbf{b}}\theta(x, y) = \frac{\pi}{Mb}$ are rotation rates along the primary axes and $\sigma = \pm 1$ is the photon spin taking the value $+1$ for RCP and -1 for LCP.

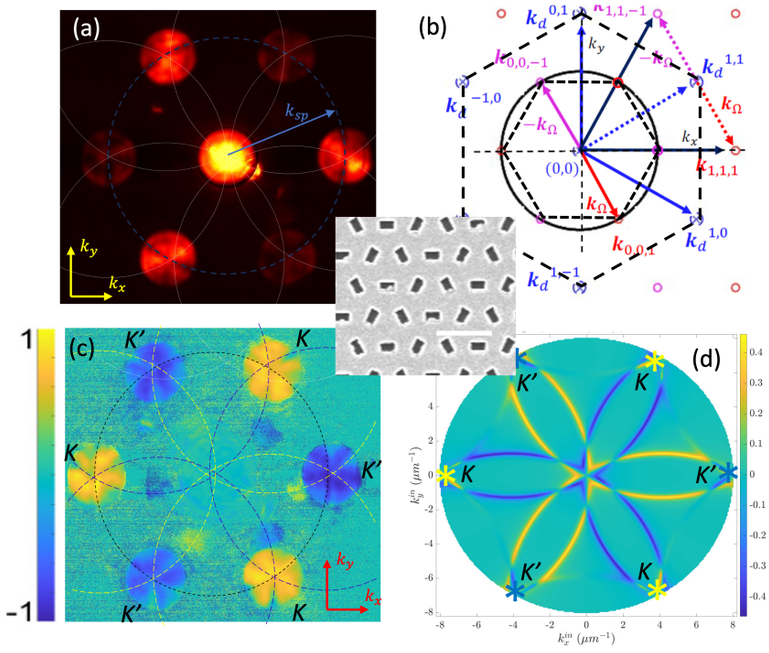

Figure 2: (a) A raw image of our measured angular intensity distribution in an ISF. The primary plasmonic resonance circle marked in blue and the secondary resonances in white. (b) Theoretically calculated k-space diagram. Blue crossed marks correspond to ODOs. Red and lavender circles correspond to RCP and LCP BOs, respectively. Solid blue arrows correspond to the reciprocal lattice vectors and solid red and lavender to the momentum of the two BOs, respectively. Dotted lines show the displacement of an ODO and its respective BOs. Solid dark blue lines denote the total optical momentum of a diffracted mode. (c) CD map of the hexagonal PB phase grating. (d) Simulated CD. The inset shows the SEM image of the hexagonal structure (a scalebar is 1 micron).

We captured a raw image of the k-space as presented in Fig. 2a. This image represents an isofrequency surface (IFS), which is essentially a slice of the three-dimensional dispersion at the laser frequency ω. The obtained diffraction pattern corresponds to the reciprocal lattice of the hexagonal structure. The circle of radius $|k_{sp}| = 2\pi/\lambda_{sp}$ (marked by the dashed line) is the plasmonic resonance representing the excitation of the SPs at the gold-air interface. The additional circular arcs are replications of the plasmonic momentum circle centered at other diffraction spots, due the grating periodicity.[30] Some of these secondary modes are marked for clarity. Points in k-space at which a diffraction spot coincides with the primary plasmonic mode represent the momentum at which the excitation of the SP occurs. Therefore, in real space, the SPs propagate in the directions determined by the momentum matching[27] (see Figs. 2(c and f)). As shown schematically in Fig. 2b, the diffraction spots coinciding with the plasmonic circle are the Berry orders (BOs) originating from the geometrical phase. The ordinary diffraction orders (ODOs) resulting from the periodicity of the structure (disregarding the rotation of apertures) are located further away and are beyond the field of view. The inner hexagonal dashed line marks the edge of the first Brillouin zone (FBZ) with the K and K' points coinciding with BOs. Measuring for both polarization states, we obtain the CD map shown in Fig. 2c. The map indicates that the secondary modes centered

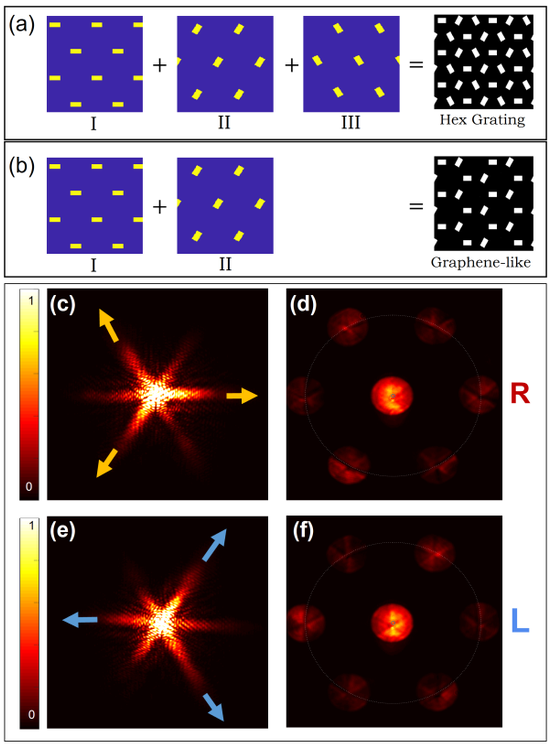

Figure 3: (a) Illustration of decomposition of the hexagonal grating into three larger hexagonal sub-lattices. (b) Superposition of only two sub-lattices gives our graphene-like metasurface. Correspondence between k-space and real space. (c),(d) Real and k-space images respectively for RCP light. The three brighter diffraction spots coinciding with the plasmonic circle in (d) correspond to the three stronger plasmonic beams propagating in real space in (c). (e) and (f) The same as (c) and (d) for LCP light.

at the K and K' points maintain the polarization of the corresponding BO. We confirm this by the simulated CD map (Fig. 2d) where the plasmonic modes are traced throughout the FBZ using a scattering formalism based on the coupled waveguidemode method.[31] We conclude that the presented hexagonal PB phase structure has a strong spin dependence manifested in the diffraction pattern and the secondary plasmonic modes.

Now we consider this hexagonal PB phase structure as a superposition of three sub-lattices of non-rotating apertures (I,II and III). Each sub-lattice has a period of $3a$, a displacement a between them and is rotated $60°$ with respect to one another (Fig. 3a). A uniform orientation of the apertures in each structure leads to a uniform PB phase, however combining all the structure with their respective phases reveals the expected polarization-dependent behavior. When one of the sub-lattices is removed (here we remove III), the structure becomes a graphene-like metasurface with lattice constant $a = 2\lambda/3$ and relative angle $\theta = \pi/3$ (Fig. 3b). As can be seen, the efficiency of the BOs is degraded and the spin-degeneracy that was lifted, reappears. Nevertheless, the broken space-inversion symmetry of the structure still results in spin-dependent directionality. Both real and k-space measurements of such a structure show the described behavior (Fig. 3 (c-f)). The weaker polarization contrast can be linked to the PB phase discontinuity due to the missing sub-lattice. However, it can be compensated by varying the relative angle between the two remaining

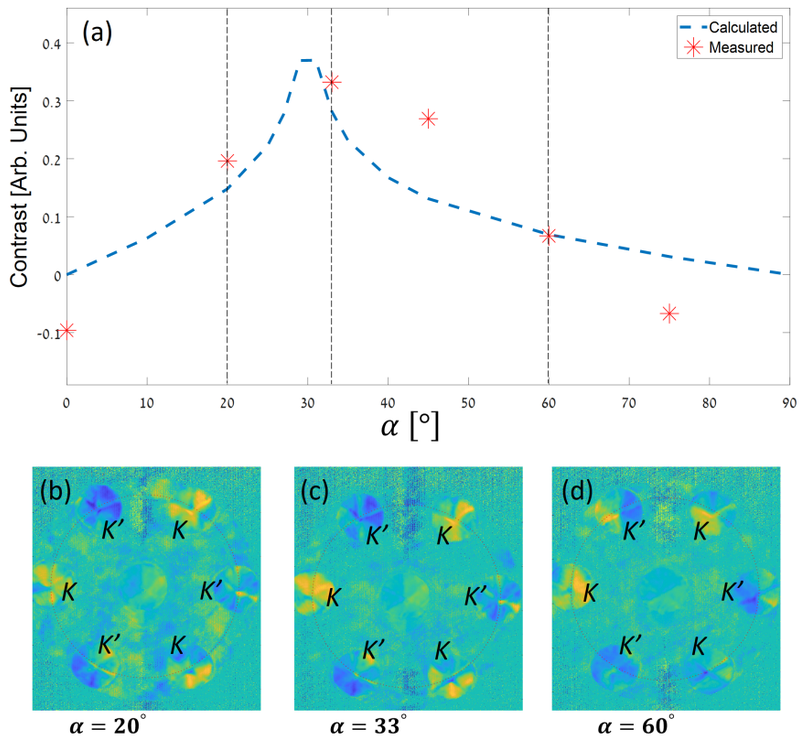

Figure 4: (a) Measured intensity contrast between diffraction orders excited with different circular polarizations as a function of the relative angle between the two sub-lattices. (b)-(d) Measured k-space CD maps for angles $20°, 33°, 60°$.

sub-lattices. We fabricated a total of 6 structures with different relative angles and measured the CD maps in the k-space (Eq. 1). From the CD, we calculated and plotted the polarization contrast between the orders at points K and K' and the relative angle α (Fig. 4a). For comparison, we used a simple model based on Huygens' principle to simulate the momentum space distribution of the SP waves excited by the sub-lattices with a PB phase difference of $2\sigma\theta(x, y)$ (dashed line in Fig.4a).

We found that in the full range of scanned angles (from $0°$ to $90°$), the measured points showed a qualitative correspondence to the model prediction with a peak contrast around $33°$. When the relative angle tends to $0°$ or $90°$, the structure becomes spin-degenerate (as expected) and the polarization contrast diminishes. This confirms that the PB phase acquired by the SP waves is the main effect responsible for the spin-dependent directional excitation of our graphene-like metasurface. Again, the polarization selectivity in the K and K' directions is reminiscent of the spin-dependent valleys in the characteristic dispersion of the TMDs. We made further important observations by investigating the CD maps of structures with different α (Fig. 4(b-d)). We found that the diffraction spots of the structure with $\alpha = 33°$ exhibiting the maximum contrast (Fig. 4c) had rather uniform CD, similar to the hexagonal structure (Fig. 2c). Away from the peak angle, we noted that the polarization of the orders located at K and K' points became space-variant. Interestingly, this behavior is also imprinted in the corresponding plasmonic modes. Figure 5a shows the measured

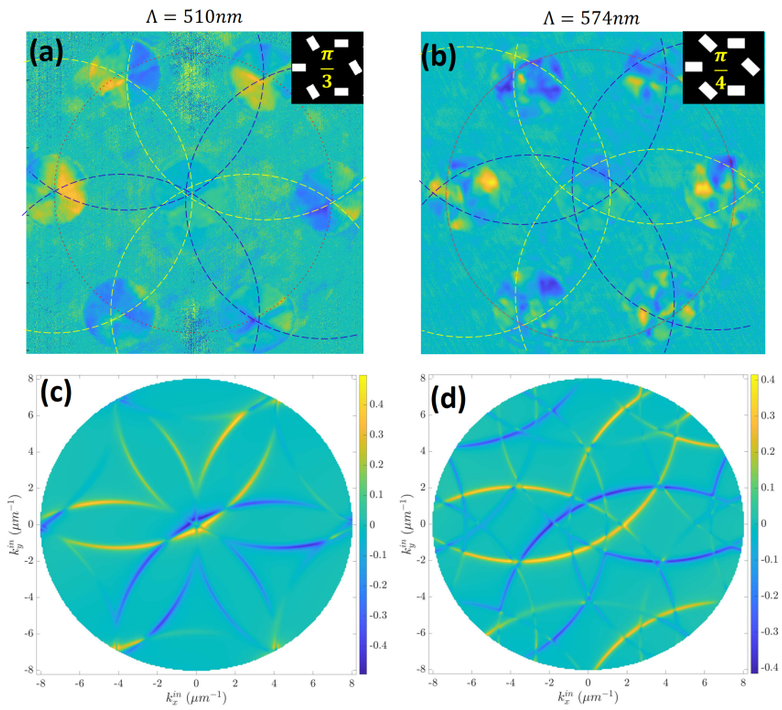

Figure 5: Measured CD maps in of graphene-like structure with a lattice constant $a = 510$ nm (a) and $a = 574$ nm (b) showing space-variant polarization. (c) and (d) Simulated CD maps for given periods.

and calculated IFS CD map behind the structure with a lattice constant $a = 510$ nm and $\theta = \pi/3$. It appears from the color-coding that the polarization exciting each of the plasmonic mode rings varies strongly along the azimuthal direction. The effect becomes more pronounced when the structure period is increased to $a = 574$ nm (Fig. 5(b,d)) and the angle is set to $\theta = \pi/4$. Our measured and calculated maps indicate the polarization state of the absorption in the k-space; therefore, one can regard our structure as a resonant space-variant polarizer. This optical manipulation can be conveniently mapped as a closed path on a Poincaré sphere, resulting in the geometric Berry phase. By following the calculated plasmonic modes, we indeed noticed a winding phase within each diffraction spot which appeared to be a function of structure period and the relative angle. When we examined the raw k-space images measured with the latter structures ($a = 574$ nm and $\alpha = \pi/4$), we recognized a dark spot in the center of each diffraction spot, which, we propose, arose from the aforementioned phase singularity. We compared this distribution with the one measured from the full hexagonal structure but illuminated with a laser beam decorated by a spiral phase (Fig.6). The similarities between the images led us to the conclude that our graphene-like structure (shown in Fig. 1) induces an optical vortex in each diffraction order. It appears that turning a hexagonal grating into a graphene-like structure by subtracting one of the three comprising sub-lattices makes a fundamental change in the behavior of the SPs. First, as can be seen in Fig. 6 each of the six apertures in a graphene-like unit-cell has only three neighbors in a contrast with six neighbors in the hexagonal one. This clearly reduces the plasmonic hopping mobility in the array leading to

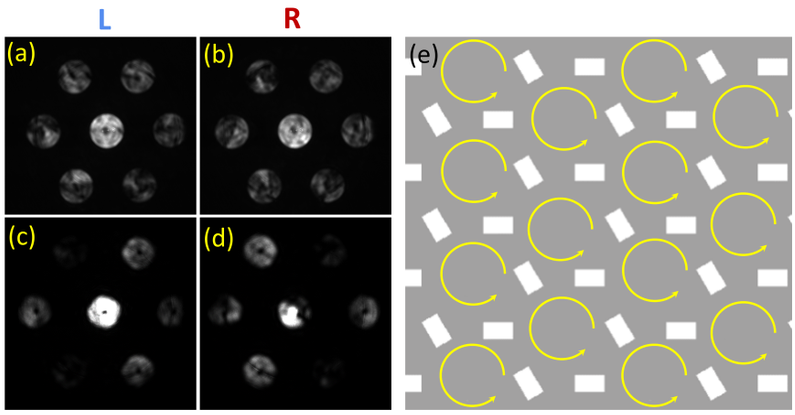

Figure 6: The comparison of the measured k-space distributions for the structure with $a = 574$ nm and $\alpha = \pi/4$ with RCP and LCP illumination (a) and (b) and for the hexagonal structure decorated with a spiral phase with $a = 510$ nm with RCP and LCP illumination (c) and (d). The schematic plasmonic hopping circulation is shown in (e).

band-gap opening along the primary axes. Accordingly, the SP wave is forced to circulate between the closest neighbors in the unit-cell. When the apertures of the array are rotated, the unit-cell becomes chiral, which lifts the degeneracy between the two counter circulating plasmonic modes, giving rise to a favorable vorticity. Summing up the local unit-cell bound SP vortices results in our case in an overall topological Berry phase along the edge of the whole structure seen in Fig. 1 as an edge state. This polarization dependent plasmonic mode is induced by a space-inversion symmetry breaking in the structure in analogy with a variety of recently presented topological insulators.

3.1 Research plan and metodology

Our preliminary results show that space-inversion symmetry in graphene-like plasmonic metasurfaces leads to strong polarization dependent directionality on SP modes and under some conditions results in a spin-dependent edge state. These effects have been recently demonstrated with excitonic modes in TMDs. Further study of our proposed structures may shed light on the fundamental aspects of topological phases both in solid-state physics and in photonics, providing a vast range of possible nanophotonic applications. Accordingly, our research plan determined by the objectives presented in section 2 suggests achieving the following aims.

3.2 Establishing a solid connection between the structure geometry and the spin-dependent plasmonic effects

We intend to perform a systematic study of a variety of plasmonic structures possesing space-inversion symmetry breaking. In addition to few structures presented in the previous section, we wish to extend these experiments with different lattice constants, aperture parameters and illumi-

nations to obtain a full understanding of the underlying physical mechanisms leading to the spin-dependent plasmonic propagation. We also propose to elaborate a theoretical model that could predict these effects and explain the analogy with the 2D materials such as TMDs or Graphene.

3.3 Verification of the helical phase

As stated in the Working Hypothesis, the transition from the hexagonal grating to the graphene-like structure brings about a fundamental change in the physical behaviour of the structure. One of the direct outcomes is the spatially varying phase acquired in each of the diffracted PB orders. As stated in the previous section, this phase is suggested to be a result of unit-cell chirality. We propose to actually verify this phase through a direct measurement and by means of a numerical and a semi-analytical calculations. Previously, we constructed a leakage radiation microscopy embedded in a Mach-Zehnder interferometer to obtain an instantaneous phase of a plasmonic signal (Fig. 7). This has been earlier used to track the propagation in time of ultra-short plasmonic pulses.[32] We

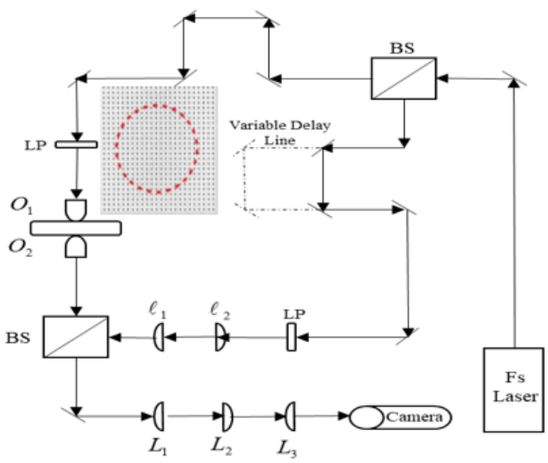

Figure 7: Hetrodyne system based on a Mach-Zehnder interferometry for time-resolved plasmonic pulse tracking.

propose to modify this setup to conveniently capture the phases of different diffraction orders in the k-space. In order to do this we propose to expand the reference beam to allow for the interference with the k-space image. These measurements can provide the connection between the structure configuration and geometry and the resulting topological phases.

In parallel we intend to study the unit cell of different structure with Comsol Multiphysics software. We propose to ”illuminate” the structure by light with a specific polarization and frequency and follow the behaviour of the excited plasmon mode phase. These results can then be compared with the ones obtained experimentally.

3.4 Realizing topological metasurface based on chiral unit-cell array

We propose to investigate more plasmonic structures, potentially leading to the appearance of edge states, topological phases and spin-dependent behavior. Using the space-inversion symmetry as a trigger for spin-orbit coupling, we propose using arrays with chiral apertures (Fig. 8). We believe that the chirality would influence the overall topological phase of the domain and pro-

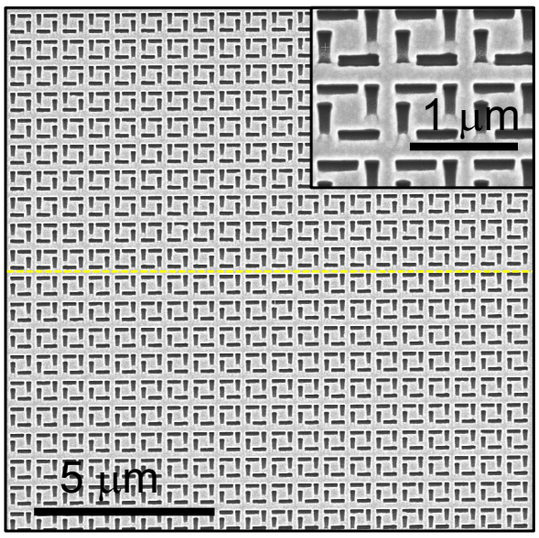

Figure 8: SEM image of the fabricated chiral metasurface. The unit cell here comprises of 4 rectangles arranged in a chiral way with a broken mirror symmetry (see the inset). The handedness of the unit cell in the upper part is opposite to the one in the lower part (a dashed line separates the domains).

vide an additional means for light manipulation. Specifically, we propose that each unit cell of the structure induces chiral plasmonic near-fields, resulting in an overall topological phase. We have already investigated similar structures with constant or space-variant chirality that have shown strong polarization-dependent behavior and may be good candidates for topology based plasmonics.[33] We intend to investigate the behavior of plasmonic waves in structural ”domains“ with opposite handedness, which could lead to the topological states.

3.5 Combining plasmonic metasurfaces with a TMD layer

Considering the models and the experimental results achieved up to this point we suggest to combine the plasmonic structure with a broken space-inversion symmetry with a TMD layer. Our investigation in this stage will be focused on enhancement of spin-orbit coupling in the system which may result in a strong coupling effect. This effect has been observed in one-dimentional grating some time ago. Nevertheless, a plasmonic structure with similar symmetry as the TMD crystal may lead to intriguing behaviours that have not been observed before.

3.6 Proposing practical applications

Some practical applications for sensing, optical communication, computing, and nanophotonic circuitry will be proposed and experimentally tested. The proposed plasmonic metasurfaces and the fundamental concepts may play a crucial role in understanding complex physical mechanisms that govern the optical spin-orbit interaction and topological photonics as well as opening new opportunities in nanotechnology development.

3.7 Current research infrastructure

Our nanooptics lab in Ariel University posses the following equipment

- High Resolution Sputter Coater equipped with QCM thickness meter (used for gold layer evaporation)
- Preheated sonication bath (used for sample and glassware cleaning)
- Drying oven (2501) with air circulation mechanism (used for drying clean samples)
- Pigtail CW laser (Ao = 780nm, 20mW power) (used as the illumination source)
- C-Fiber 780 femtosecond Erbium laser (λ= 780nm, pulse duration - 70 fs average power - lOOmW – used as an additional illumination source, especially for time-resolved or phase resolved measurements)
- Polarizing elements (for full polarization control of the illumination and beam analysis)
- Optics free space elements (for beam shaping filtering aligning and manipulating)
- Number of CMOS and CCD based cameras (for image acquisition)
- Computers (for collecting data and controlling the optical elements as well as for model calculation and simulation)
- Olympus microscope (for sample inspection)
- Optical dry and oil immersion objectives (for imaging and illumination of samples)

Resources outside of Ariel University

- Bar-Ilan university nanofabrication facilities – for nanofabrication of our samples

Human resources currently affiliated with the project

- Eliav Epstein – research fellow (Graduated with PhD, January 2021)
- Pasha Goz – PhD student (finishes February 2027)
- Sahil Sahoo – PhD student (finishes October 2027)

3.8 Expected Outcomes and Pitfalls

We will start with the investigation of SP wave propagation in lattices with broken space-inversion symmetry as discussed in Research Plan and Preliminary Results. While the preliminary results are convincing, more experimental data should be obtained to verify our hypothesis and conclusions. In particular we plan to perform a full numerical study of the photonic band-gap structure of our metasurfaces and compare the results obtained with the graphene-like unit-cell and the hexagonal structure. By manipulating the periodicity, orientation angle and other parameters, we plan to achieve various topological phases in K and K' points. This could provide a means for topologically based plasmonic mode manipulation. We expect to summarize our results and further investigations in 7 to 9 high-impact factor papers within the period of the three years. Although some of the expected results have been partially verified in our lab the future investigation will have to deal with rather complex experimental settings and nanofabrication challenges. We have much experience in both of these areas, nevertheless we take into account the following possible pitfalls.

i Fabrication irregularities. Our structures are fabricated by FIB in a gold film evaporated on glass slide. We expect some errors and misalignments that can reduce repeatability of the measurements. We therefore plan to optimize and stabilize the fabrication process as well as find the optimal structural parameters in order to bring these errors to the minimum.

ii Model convergence. Since our theory will be verified by the semi-analytical Matlab solver and by a commercial software, one may expect non-convergence of these two models and even some contradiction. This will teach us about possible errors in some of our assumptions which will have to be corrected.

iii Heterostructure fabrication and testing. We plan to study a system comprised of a plasmonic metasurface covered by a TMD material. This may impose some technical issues and lead to the measurement difficulties. The fabrication processes then will have to be updated to achieve the best possible results.

Bibliography

[1] N. Mounet, M. Gibertini, P. Schwaller, D. Campi, A. Merkys, A. Marrazzo, T. Sohier, I. E. Castelli, A. Cepellotti, G. Pizzi, *et al.*, “Two-dimensional materials from high-throughput computational exfoliation of experimentally known compounds,” *Nature Nanotechnology*, vol. 13, no. 3, pp. 246–252, 2018.

[2] S. Z. Butler, S. M. Hollen, L. Cao, Y. Cui, J. A. Gupta, H. R. Gutiérrez, T. F. Heinz, S. S. Hong, J. Huang, A. F. Ismach, *et al.*, “Progress, challenges, and opportunities in two-dimensional materials beyond graphene,” *ACS Nano*, vol. 7, no. 4, pp. 2898–2926, 2013.

[3] S. Manzeli, D. Ovchinnikov, D. Pasquier, O. V. Yazyev, and A. Kis, “2d transition metal dichalcogenides,” *Nature Reviews Materials*, vol. 2, no. 8, pp. 1–15, 2017.

[4] G. Wang, A. Chernikov, M. M. Glazov, T. F. Heinz, X. Marie, T. Amand, and B. Urbaszek, “Colloquium: Excitons in atomically thin transition metal dichalcogenides,” *Reviews of Modern Physics*, vol. 90, no. 2, p. 021001, 2018.

[5] A. Gupta, T. Sakthivel, and S. Seal, “Recent development in 2d materials beyond graphene,” *Progress in Materials Science*, vol. 73, pp. 44–126, 2015.

[6] J. R. Schaibley, H. Yu, G. Clark, P. Rivera, J. S. Ross, K. L. Seyler, W. Yao, and X. Xu, “Valleytronics in 2d materials,” *Nature Reviews Materials*, vol. 1, no. 11, pp. 1–15, 2016.

[7] F. Wu, T. Lovorn, E. Tutuc, I. Martin, and A. MacDonald, “Topological insulators in twisted transition metal dichalcogenide homobilayers,” *Physical Review Letters*, vol. 122, no. 8, p. 086402, 2019.

[8] X. Li, S. Zhang, and Q. Wang, “Topological insulating states in 2d transition metal dichalcogenides induced by defects and strain,” *Nanoscale*, vol. 9, no. 2, pp. 562–569, 2017.

[9] M. V. Berry, “Quantal phase factors accompanying adiabatic changes,” *Proceedings of the Royal Society of London. A. Mathematical and Physical Sciences*, vol. 392, no. 1802, pp. 45–57, 1984.

[10] D. Xiao, M.-C. Chang, and Q. Niu, “Berry phase effects on electronic properties,” *Reviews of Modern Physics*, vol. 82, no. 3, p. 1959, 2010.

[11] J. Segert, “Photon berry’s phase as a classical topological effect,” *Physical Review A*, vol. 36, no. 1, p. 10, 1987.

[12] K. Y. Bliokh, A. Niv, V. Kleiner, and E. Hasman, “Geometrodynamics of spinning light,” *Nature Photonics*, vol. 2, no. 12, pp. 748–753, 2008.

[13] L. Lu, J. D. Joannopoulos, and M. Soljačić, “Topological photonics,” *Nature Photonics*, vol. 8, no. 11, pp. 821–829, 2014.

[14] J. D. Joannopoulos, P. R. Villeneuve, and S. Fan, “Photonic crystals,” *Solid State Communications*, vol. 102, no. 2-3, pp. 165–173, 1997.

[15] E. Yablonovitch, “Inhibited spontaneous emission in solid-state physics and electronics,” *Physical Review Letters*, vol. 58, no. 20, p. 2059, 1987.

[16] S. Pancharatnam, “Generalized theory of interference and its applications,” in *Proceedings of the Indian Academy of Sciences-Section A*, vol. 44, pp. 398–417, Springer, 1956.

[17] M. V. Berry, “The adiabatic phase and pancharatnam’s phase for polarized light,” *Journal of Modern Optics*, vol. 34, no. 11, pp. 1401–1407, 1987.

[18] K. Y. Bliokh and Y. P. Bliokh, “Topological spin transport of photons: the optical magnus effect and berry phase,” *Physics Letters A*, vol. 333, no. 3-4, pp. 181–186, 2004.

[19] C. McDonnell, J. Deng, S. Sideris, T. Ellenbogen, and G. Li, “Functional thz emitters based on pancharatnam-berry phase nonlinear metasurfaces,” *Nature Communications*, vol. 12, no. 1, pp. 1–8, 2021.

[20] S. Liu, S. Qi, Y. Li, B. Wei, P. Li, and J. Zhao, “Controllable oscillated spin hall effect of bessel beam realized by liquid crystal pancharatnam-berry phase elements,” *Light: Science & Applications*, vol. 11, no. 1, p. 219, 2022.

[21] Z. Bomzon, G. Biener, V. Kleiner, and E. Hasman, “Space-variant pancharatnam–berry phase optical elements with computer-generated subwavelength gratings,” *Optics Letters*, vol. 27, no. 13, pp. 1141–1143, 2002.

[22] K. Y. Bliokh, Y. Gorodetski, V. Kleiner, and E. Hasman, “Coriolis effect in optics: unified geometric phase and spin-hall effect,” *Physical Review Letters*, vol. 101, no. 3, p. 030404, 2008.

[23] K. Y. Bliokh, “Geometrical optics of beams with vortices: Berry phase and orbital angular momentum hall effect,” *Physical Review Letters*, vol. 97, no. 4, p. 043901, 2006.

[24] Y. Gorodetski, A. Niv, V. Kleiner, and E. Hasman, “Observation of the spin-based plasmonic effect in nanoscale structures,” *Physical Review Letters*, vol. 101, no. 4, p. 043903, 2008.

[25] L. Huang, X. Chen, B. Bai, Q. Tan, G. Jin, T. Zentgraf, and S. Zhang, “Helicity dependent directional surface plasmon polariton excitation using a metasurface with interfacial phase discontinuity,” *Light: Science & Applications*, vol. 2, no. 3, pp. e70–e70, 2013.

[26] J. Lin, J. B. Mueller, Q. Wang, G. Yuan, N. Antoniou, X.-C. Yuan, and F. Capasso, “Polarization-controlled tunable directional coupling of surface plasmon polaritons,” *Science*, vol. 340, no. 6130, pp. 331–334, 2013.

[27] M. Fox and Y. Gorodetski, “Generalized approach to plasmonic phase modulation in topological bi-gratings,” *Applied Physics Letters*, vol. 120, no. 3, p. 031105, 2022.

[28] L. Feng, R. El-Ganainy, and L. Ge, “Non-hermitian photonics based on parity–time symmetry,” *Nature Photonics*, vol. 11, no. 12, pp. 752–762, 2017.

[29] A. Drezet, A. Hohenau, D. Koller, A. Stepanov, H. Ditlbacher, B. Steinberger, F. R. Aussenegg, A. Leitner, and J. R. Krenn, “Leakage radiation microscopy of surface plasmon polaritons,” *Materials Science and Engineering: B*, vol. 149, no. 3, pp. 220–229, 2008.

[30] E. D. Epstein, L. Singh, S. Sternklar, and Y. Gorodetski, “The role of plasmonic excitations in the optical activity of periodic structures with configurational chirality,” *Applied Physics Letters*, vol. 116, no. 13, p. 131106, 2020.

[31] F. Lorén, G. L. Paravicini-Bagliani, S. Saha, J. Gautier, M. Li, C. Genet, and L. Martín-Moreno, “Microscopic analysis of spin-momentum locking on a geometric phase metasurface,” *Physical Review B*, vol. 107, no. 16, p. 165128, 2023.

[32] Y. Gorodetski, T. Chervy, S. Wang, J. A. Hutchison, A. Drezet, C. Genet, and T. W. Ebbesen, “Tracking surface plasmon pulses using ultrafast leakage imaging,” *Optica*, vol. 3, no. 1, pp. 48–53, 2016.

[33] L. Singh, M. Fox, S. Sternklar, and Y. Gorodetski, “Topological diffraction from grating with space variant chirality,” *ACS Photonics*, vol. 9, no. 4, pp. 1395–1399, 2022.